Mechanism of Associatively Controlled Ligand Substitution in Square-Planar Bis(*N*-alkylsalicylaldiminato)nickel(II) Complexes: Kinetic, Spectroscopic, and Thermodynamic Characterization of Adducts and Intermediates

Harald Hoss and Horst Elias*

Anorganische Chemie III, Eduard-Zintl-Institut der Technischen Hochschule Darmstadt, D-6100 Darmstadt, Germany

Received June 19, 1992

Spectrophotometric titration was used to determine the equilibrium constants and thermodynamic parameters $\Delta H°$ and $\Delta S°$ for the addition of mono- and bidentate N-bases to planar four-coordinate complexes I = bis(*N*-ethylsalicylaldiminato)nickel(II), II = bis(*N*-ethyl-5-nitrosalicylaldiminato)nickel(II), III = bis(*N*-*n*-propyl-5-nitrosalicylaldiminato)nickel(II), and IV = bis(*N*-ethyl-3-nitro-5-*tert*-butylsalicylaldiminato)nickel(II) in the solvent acetone. The visible absorption properties of the base adducts are reported. Single-wavelength and multiwavelength stopped-flow spectrophotometry was applied to study the displacement of the two bidentate ligands in I and II by tetradentate ligands H_2salen = *N*,*N*′-disalicylideneethylenediamine, H_2[H_4]salen = *N*,*N*′-bis(2-hydroxybenzyl)-1,2-diaminoethane, and H_2BuMe[H_4]salen = *N*,*N*′-bis(2-hydroxy-3-*tert*-butyl-5-methylbenzyl)-1,2-diaminoethane in acetone at ambient and reduced temperature. Rate laws and activation parameters $\Delta H^{\ddagger}$ and $\Delta S^{\ddagger}$ for the various substitution reactions are reported. The kinetic and spectroscopic results prove that substitution is initiated by the formation of the adducts (I·H_2B) and (II·H_2B), with H_2B = H_2salen, H_2[H_4]salen, or H_2BuMe[H_4]salen. It follows from the spectroscopic and thermodynamic properties of these adducts that the nickel is six-coordinate, the tetradentate ligands H_2B being coordinated in a bidentate fashion through the two nitrogen atoms. The kinetic parameters describing the mono- or biphasic decay of the initially formed adducts to products are presented, and a three-step mechanism for ligand substitution is discussed.

Introduction

It is generally accepted that the key pathway for ligand substitution in square-planar, four-coordinate complexes with d^8 metal centers such as Pt(II), Pd(II), Ni(II), Ir(I), and Au(III) is a second-order reaction between the complex and the entering nucleophile with an associative mode of activation (A mechanism).[1] In this process, both bond-making and bond-breaking are involved in the formation of the coordinatively expanded intermediate (ML_3XY) according to (1). From the kinetic point

$$ML_3X + Y \overset{K}{\rightleftharpoons} (ML_3XY) \overset{k}{\rightarrow} ML_3Y + X \qquad (1)$$

of view, the rate law expected for excess conditions ($[ML_3X]_0 \ll [Y]_0$), rate = k_{obsd}[complex], is of the saturation type, with $k_{obsd} = kK[Y]/(1 + K[Y])$. Examples of the full associative rate law (i.e., with saturation being observable) are rare,[2] however, because the postulated intermediate must be quite stable if $K[Y] \geq 1$. Coordinatively unsaturated systems are most likely to satisfy this condition.

Our recent work[3,4] on the kinetics and mechanism of ligand substitution in square-planar bis(*N*-alkylsalicylaldiminato)-nickel(II) complexes Ni(R-sal)$_2$ by salen and salen derivatives H_2B in acetone according to (2) led to a second-order rate law

$$Ni(R\text{-}sal)_2 + H_2B \rightleftharpoons NiB + 2R\text{-}salH \qquad (2)$$

for the substitution, rate = k_2[complex][H_2B], and provided convincing experimental evidence for the operation of an A mechanism. With a given complex, any variation in the attacking ligand H_2B was reflected in the size of rate constant k_2 and the introduction of chirality in both H_2B and Ni(R-sal)$_2$ proved chiral discrimination to occur in the reaction of the corresponding enantiomers.[4] Nevertheless, even at very high excess concentrations of H_2B ($[H_2B]_{max}$ = 0.1 M; $[H_2B]/[complex]$ = 200–300), the experimental rate constant k_{obsd} still increased linearly with $[H_2B]_0$ without any indication of saturation, i.e. formation of an intermediate.

The present study of reaction 2 involves the complexes Ni(R-sal)$_2$ = I–IV[5] and the ligands H_2B = H_2salen, H_2[H_4]salen, and H_2BuMe[H_4]salen[5] (see Chart I). It was undertaken to further approach the question of intermediate formation in several ways, namely by increasing the Lewis acidity of the nickel center in Ni(R-sal)$_2$, by raising the base strength of the entering ligand H_2B, by investigating adduct formation according to (3) with a

$$Ni(R\text{-}sal)_2 + B \overset{K_1}{\rightleftharpoons} Ni(R\text{-}sal)_2 \cdot B \qquad (3)$$

variety of bases B, and by following reaction 2 at low temperatures. This approach was successful in the sense that it allowed a detailed kinetic, spectroscopic, and thermodynamic study of the formation and decay of the expected intermediate (Ni(R-sal)$_2$$H_2$B).

Experimental Section

Solvent and Reagents. Acetone (Merck; analytical grade) was used for the kinetic runs without further purification. The following compounds were purchased (98–99% purity): ethylenediamine, methylamine (aqueous solution), ethylamine, *n*-propylamine, pyridine, pyridine-2-carbox-

(1) Wilkins, R. G. *Kinetics and Mechanism of Reactions of Transition Metal Complexes*, 2nd ed.; VCH: Weinheim, Germany, 1991; p 234.
(2) Jordan, R. B. *Reaction Mechanisms of Inorganic and Organometallic Systems*; Oxford University Press: Oxford, U.K., 1991; pp 41–43.
(3) Schumann, M.; Elias, H. *Inorg. Chem.* **1985**, *24*, 3187.
(4) Warmuth, R.; Elias, H. *Inorg. Chem.* **1991**, *30*, 5027.

(5) Abbreviations: Ni(Et-sal)$_2$ = bis(*N*-ethylsalicylaldiminato)nickel(II), Ni(Et-NO_2sal)$_2$ = bis(*N*-ethyl-5-nitrosalicylaldiminato)nickel(II), Ni(Pr-NO_2sal)$_2$ = bis(*N*-*n*-propyl-5-nitrosalicylaldiminato)nickel(II), Ni(Et-NO_2Busal)$_2$ = bis(*N*-ethyl-3-nitro-5-*tert*-butylsalicylaldiminato)-nickel(II), H_2salen = *N*,*N*′-disalicylideneethylenediamine, H_2[H_4]salen = *N*,*N*′-bis(2-hydroxybenzyl)-1,2-diaminoethane, H_2BuMe[H_4]salen = *N*,*N*′-bis(2-hydroxy-3-*tert*-butyl-5-methylbenzyl)-1,2-diaminoethane, py = pyridine, bpy = 2,2′-bipyridine, Et_2en = *N*,*N*′-diethylethylenediamine, MeNBu = *N*-methyl-*n*-butylamine, MeIm = *N*-methylimidazole, PrPA = 2-(2-aza-1-pentenyl)pyridine, PrBA = *N*-*n*-propylbenzaldimine.

0020-1669/93/1332-0317$04.00/0

Chart I

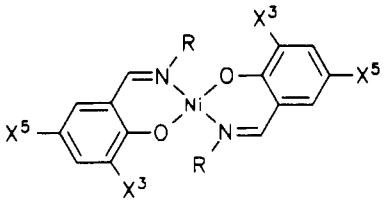

$Ni(R\text{-}X^3X^5sal)_2$

Complex[5]	R	X^3	X^5
I = $Ni(Etsal)_2$	Et	H	H
II = $Ni(Et\text{-}NO_2sal)_2$	Et	H	NO_2
III = $Ni(Pr\text{-}NO_2sal)_2$	nPr	H	NO_2
IV = $Ni(Et\text{-}NO_2Busal)_2$	Et	NO_2	tBu

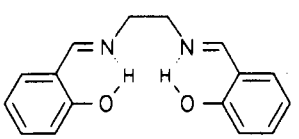

H_2salen

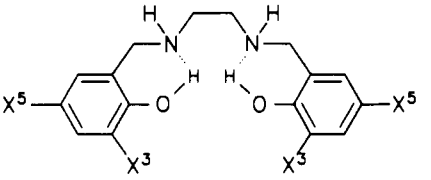

$H_2[H_4]salen$ (X^3=X^5=H)

$H_2BuMe[H_4]salen$ (X^3=tBu, X^5=Me)

aldehyde, 2,2′-bipyridine, 4-*tert*-butylphenol, 2-*tert*-butyl-4-methylphenol, benzaldehyde, salicylaldehyde, 5-nitrosalicylaldehyde.

Aldehydes, Schiff Bases, and Ligands. 3-Nitro-5-*tert*-butylsalicylaldehyde was prepared from 4-*tert*-butylphenol by formylation[6] and subsequent nitration.[7] The Schiff bases *N*-ethylsalicylaldimine, 2-(2-aza-1-pentenyl)pyridine (from pyridine-2-carboxaldehyde and *n*-propylamine), *N*-ethyl-5-nitrosalicylaldimine, *N*-*n*-propyl-5-nitrosalicylaldimine, and *N*-ethyl-3-nitro-5-*tert*-butylsalicylaldimine were prepared by reaction of the aldehyde with the corresponding amine (10% excess) in methanol as described earlier.[8] A slightly different procedure[9] was applied for the preparation of the Schiff base *N*-*n*-propylbenzaldimine. The yellow imines were purified by either recrystallization or distillation in vacuo.

The ligand H_2salen[5] was prepared from ethylenediamine and salicylaldehyde[4] and hydrogenated with $NaBH_4$ in methanol to obtain colorless crystals[10] of tetrahydrosalen = $H_2[H_4]salen$.[5] The preparation of $H_2BuMe[H_4]salen$[5] was described recently.[11]

Complexes. The nickel complex I was prepared from $Ni(sal)_2 \cdot 2H_2O$ (=bis(salicylaldehydato)nickel(II) dihydrate) and ethylamine according to a procedure described earlier,[12] whereas complex III was obtained as published by Holm.[13] The following procedure was used to prepare complexes II and IV: To a hot solution of the corresponding Schiff base ligand (0.05 mol) in MeOH (50 mL) was slowly added a solution of NaOAc (0.06 mol) and $Ni(OAc)_2 \cdot 4H_2O$ (0.025 mol) in MeOH (50 mL) under stirring. The complex precipitated immediately, was separated by filtration, and was recrystallized from MeOH (II) and *i*-PrOH (IV), respectively.

The green complexes I–IV and the ligands $H_2[H_4]salen$ and $H_2BuMe[H_4]salen$ were characterized by elemental analysis, the results being in good agreement with the calculated data.

Instrumentation. UV/vis spectra: diode array spectrophotometer (Hewlett-Packard, Type 8541). Slow kinetics: double-beam spectrophotometer (Varian, Type DMS 300). Fast kinetics: modified[14] stopped-flow spectrophotometer (Durrum, D 110) and rapid-scan–stopped-flow spectrophotometer, in combination with a cryostat (−90 to +30 °C), as described earlier.[15,16]

Spectrophotometric Titration. The titration of the acetone solutions of complexes $Ni(R\text{-}sal)_2 = NiA_2$ with bases B according to (3) or (4) was

$$NiA_2 + 2B \overset{K_1}{\rightleftharpoons} NiA_2 \cdot B + B \overset{K_2}{\rightleftharpoons} NiA_2 \cdot 2B \qquad (4)$$

followed spectrophotometrically. The absorbance/[B] data for a given wavelength were computer-fitted to eq 5 of this contribution or to eq 5,

$$A = \{A^\circ(NiA_2) + (A^\circ(NiA_2 \cdot B)K_1[B]\}/(1 + K_1[B]) \qquad (5)$$

given in ref 12, to obtain K_1 and K_2. The symbols $A^\circ(NiA_2)$ and $A^\circ(NiA_2 \cdot B)$ refer to the absorbance of the species NiA_2 and $NiA_2 \cdot B$ at a concentration of $[Ni]_{tot}$.

Kinetic Measurements. Reaction 2 was followed by spectrophotometry (conventional, stopped-flow or rapid-scan–stopped-flow), mostly under pseudo-first-order conditions ($[complex]_0 \ll [H_2B]_0$). The A/t data, resulting from the observed decrease or increase in absorbance A with time t, were computer-fitted to either eq 6 (irreversible first-order reaction)

$$A = (A_0 - A_\infty)[\exp(-k_{obsd}t)] + A_\infty \qquad (6)$$

$$A = a_1[\exp(-k_{ob(1)}t)] + a_2[\exp(-k_{ob(2)}t)] + A_\infty \qquad (7)$$

or eq 7 (irreversible biphasic consecutive reaction). Some experiments were carried out under stoichiometric conditions ($[complex]_0 = [H_2B]_0$), and the A/t data were fitted to eq 8 (irreversible second-order reaction). The programs used were based on the least-squares method.

$$A = A_\infty + (A_0 - A_\infty)/(1 + [complex]_0kt) \qquad (8)$$

Results and Discussion

Lewis Acidity of Complexes I–IV As Studied by Adduct Formation. The vis spectra of complexes I and IV in acetone are characterized by a rather strong CT band at 414 nm (ϵ = 4700 M^{-1} cm^{-1}) and 428 nm (ϵ = 10 400 M^{-1} cm^{-1}), respectively, and a weak d–d band at 620 nm (ϵ = 70 M^{-1} cm^{-1}) and 615 nm (ϵ = 80 M^{-1} cm^{-1}), respectively. This absorption pattern is typical for square-planar bis(*N*-alkylsalicylaldiminato)nickel(II) complexes $Ni(R\text{-}sal)_2$ with a trans N_2O_2 coordination geometry and nonbranched alkyl groups such as R = ethyl and *n*-propyl.[17] The nitro group para to the phenolic oxygen causes a blue shift of the CT band to 388 nm (complex II) and 384 nm (complex III) and a considerable increase in absorption intensity (ϵ = 35 000 M^{-1} cm^{-1}). Due to the low solubility of II and III in acetone, the weak

(6) Ligget, R. W.; Diehl, H. *Proc. Iowa Acad. Sci.* **1945**, *52*, 191.
(7) Borsche, W. *Chem. Ber.* **1917**, *50*, 1339.
(8) Reiffer, U.; Schumann, M.; Wannowius, K. J.; Elias, H. Transition *Met. Chem. (London)* **1980**, *5*, 272.
(9) Zaunschirm, H. *Liebigs Ann. Chem.* **1886**, *245*, 279.
(10) O'Connor, M. J.; West, B. O. *Aust. J. Chem.* **1967**, *20*, 2077.
(11) Böttcher, A.; Elias, H.; Müller, L.; Paulus, H. *Angew. Chem.* **1992**, *104*, 635; *Angew. Chem., Int. Ed. Engl.* **1992**, *31*, 623.
(12) Schumann, M.; von Holtum, A.; Wannowius, K. J.; Elias, H. *Inorg. Chem.* **1982**, *21*, 606.
(13) Holm, R. H. *J. Am. Chem. Soc.* **1961**, *83*, 4683.
(14) Elias, H.; Fröhn, U.; von Irmer, A.; Wannowius, K. J. *Inorg. Chem.* **1980**, *19*, 869.
(15) Wannowius, K. J.; Sattler, F.; Elias, H. *GIT Fachz. Lab.* **1985**, *29*, 1138.
(16) Röper, J.; Elias, H. *Inorg. Chem.* **1992**, *31*, 1202.
(17) Holm, R. H.; O'Connor, M. J. *Prog. Inorg. Chem.* **1971**, *14*, 241.

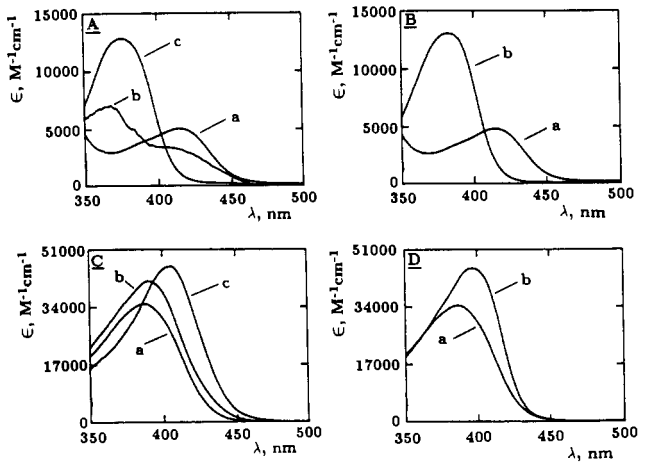

Figure 1. Vis spectra of complexes I and II and their adducts formed with various N-bases B:[5] (A) B = py, a = I, b = I·py, c = I·2py; (B) B = Et_2en, a = I, b = I·Et_2en; (C) B = MeNBu, a = II, b = II·MeNBu, c = II·2MeNBu; (D) B = Et_2en, a = II, b = II·Et_2en.

d–d band above 600 nm is hardly detectable. In agreement with the rich information available on the spectroscopic and structural properties of Ni(R-sal)$_2$ complexes,[17] the vis spectra of complexes II–IV are thus clearly indicative of square-planar trans N_2O_2 coordination geometry of the nickel.

It is well-known that planar complexes Ni(R-sal)$_2$ strongly tend to expand their coordination number, forming five- and six-coordinate species.[18] It follows from the equilibrium constants summarized in Table I that (i) complex I adds two monodentate ligands (such as py and the Schiff base PrBA) stepwise or one bidentate ligand (such as bpy, PrPA, and Et_2en) in one step to become six-coordinate, (ii) complexes II–IV show the same type of behavior, but in these complexes, due to the presence of the electron-withdrawing nitro group in the 5-position (II and III) or the 3-position of the phenyl ring (IV), the nickel center is a much better acceptor and the adducts formed are thus much more stable, (iii) amines (such as MeNBu and Et_2en) are obviously more strongly coordinated than imines (such as PrPA and also py), and (iv) a comparison of the equilibrium constants β_2 and K_1, obtained for adduct formation with the aliphatic amines MeNBu and Et_2en, respectively, clearly demonstrates the stabilizing chelate effect. Figure 1 presents the visible spectra of some of the adducts formed.[19]

One should keep in mind that the addition of cis-binding bidentate N–N ligands such as bpy or Et_2en to planar complexes Ni(R-sal)$_2$ = Ni(N–O)$_2$ necessitates a rearrangement of the two N–O ligands upon formation of the Ni(N–O)$_2$(N–N) octahedron. As a matter of fact, several isomers are to be expected for such an octahedral complex, resulting from different arrangements of the three bidentate ligands around the metal. It is worthwhile to point out therefore that the X-ray structure analysis of the adduct [Ni(Et-sal)$_2$(bpy)] proves a coordination[20] in which the four N atoms form a plane around the nickel and the two O atoms occupy axial positions.

Another point of interest is that the spectrophotometric titration of complex I with phenols (such as *N-tert*-butyl-4-hydroxybenzaldimine and phenol itself) does not lead to spectral changes indicative of phenol addition.

In conclusion, the nitro-substituted complexes II–IV are considerably stronger Lewis acids compared to complex I. In a sense, they are coordinatively unsaturated and add N-donating nucleophiles to become octahedral.

(18) See refs 3, 4, and 12 and the literature cited therein.
(19) The spectra shown are calculated ones resulting from the multiwavelength fit of the $A/[B]$ data to eq 5 of this contribution or to eq 5 given in ref 12.
(20) Viehmann, N.; Elias, H. To be published.

Table I. Equilibrium Constants for Adduct Formation from Spectrophotometric Titration of Complexes I–IV with Bases B in Acetone at 298 K According to (3) or (4)

complex[a]	base B[b] (denticity)	K_1,[c] M^{-1}	K_2,[c] M^{-1}	β_2,[c,d] M^{-2}
I = Ni(Et-sal)$_2$	py (1)	0.5	74	37
	MeNBu (1)	3.3	not obsd	not obsd
	PrBA (1)	10	8	82
	bpy (2)	470	not obsd	not obsd
	PrPA (2)	350	not obsd	not obsd
	Et_2en (2)	41 000	not obsd	not obsd
II = Ni(Et-NO_2sal)$_2$	py (1)	785	401	315 000
	MeNBu (1)	834	32	26 900
	Et_2en (2)	41 000	not obsd	not obsd
III = Ni(Pr-NO_2sal)$_2$	MeNBu (1)	1000	120	120 000
	MeIm (1)	410	23	9360
IV = Ni(Et-NO_2Busal)$_2$	py (1)	675	1150	780 000
	MeNBu (1)	2160	620	1 340 000

[a] [Complex] = 0.0001 M for I and IV and 0.000 02 M for II and III. [b] For abbreviations of bases B, see footnote 5. [c] The error in K_1, K_2, and β_2 is approximately ±10%. [d] $\beta_2 = K_1K_2$.

Kinetic Scheme Expected for Reaction 2. It is adequate to postulate that ligand substitution in Ni(R-sal)$_2$ = NiA_2 by tetradentate ligands H_2B, present in excess, takes place in three steps.

Step 1: fast equilibration with the attacking ligand to form an adduct

$$NiA_2 + H_2B \overset{K = k_1/k_{-1}}{\rightleftharpoons} (NiA_2{\cdot}H_2B) \qquad (9)$$

Step 2: loss of the first bidentate ligand and formation of an intermediate

$$(NiA_2{\cdot}H_2B) \xrightarrow{k_2} (NiAHB) + HA \qquad (10)$$

Step 3: elimination of the second bidentate ligand and formation of the product

$$(NiAHB) \xrightarrow{k_3} NiB + HA \qquad (11)$$

Depending on the system under study and the experimental conditions, different rate laws are to be expected.

Case 1, $K_1[H_2B]_0 \ll 1$ and $k_3 \gg k_2$:

$$\text{rate} = d[NiB]/dt = k_{obsd}[NiA_2] \qquad (12)$$

$$k_{obsd} = k_2K_1[H_2B]_0$$

The experimental rate constant k_{obsd} increases linearly with $[H_2B]_0$, and the slope corresponds to the product k_2K_1.

Case 2, $K_1[H_2B]_0 \geq 1$ and $k_3 \gg k_2$:

$$\text{rate} = k_{obsd}[NiA_2] \qquad (13)$$

$$k_{obsd} = k_2K_1[H_2B]_0/(1 + K_1[H_2B]_0)$$

The plot of $k_{obsd} = f([H_2B]_0)$ gives a saturation curve, from which k_1 and K_1 can be obtained by fitting.

Case 3, $K_1[H_2B]_0 \gg 1$ and $k_3 \gg k_2$:

$$\text{rate} = k_{obsd}[NiA_2]; \quad k_{obsd} = k_2 \qquad (14)$$

The experimental rate constant is independent of $[H_2B]_0$ and corresponds to k_2.

Case 4, $k_3 < k_2$ or $k_3 > k_2$: The decay of the adduct ($NiA_2{\cdot}H_2B$) to the product NiB, via the intermediate (NiAHB), is biphasic, and on the basis of eq 7, two experimental rate constants are obtained, $k_{ob(1)}$ and $k_{ob(2)}$. The experimental rate constant corresponding to k_3 will be independent of $[H_2B]_0$ under all conditions, whereas the other will follow $[H_2B]_0$ according to cases 1 (→ case 4a), 2 (→ case 4b), or 3 (→ case 4c).

Cases 2 and 4b are thus of special interest because they allow the determination of K_1 along with k_2 and k_2 plus k_3, respectively.

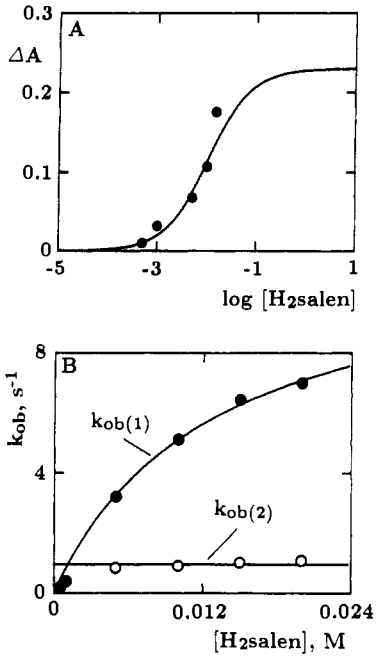

Figure 2. (A) Plot of the initial fast change in absorbance, ΔA, and (B) plot of the experimental rate constants, $k_{ob(1)}$ and $k_{ob(2)}$, vs the concentration of the entering ligand H_2salen for complex II reacting according to eq 2 in acetone at 273 K ($[II]_0 = 2 \times 10^{-5}$ M).

Kinetic Results for Complex II Reacting with Ligands H_2B. As reported earlier,[3] complex I reacts with H_2salen according to case 1 with $k_{obsd} = k_2K_1[H_2salen]_0$ and $k_2K_1 = 86.1$ M^{-1} s^{-1} at 298 K. The enhanced Lewis acidity of the nickel center in II compared to I (see Table I) led us to study reaction 2 with Ni(R-sal)$_2$ = II and H_2B = H_2salen at 273 K.[21] The kinetic pattern observed corresponds to case 4b in that (i) there is an instantaneous change in absorbance, ΔA, within the mixing time, too fast to be followed by the stopped-flow technique, and in its size dependent on $[H_2salen]_0$, (ii) product formation is biphasic, and the experimental rate constants $k_{ob(1)}$ and $k_{ob(2)}$ are obtained, and (iii) $k_{ob(1)}$ depends on $[H_2salen]_0$, and $k_{ob(2)}$ does not (see Figure 2). So, $k_{ob(2)}$ corresponds unambiguously to k_3 and $k_{ob(1)}$ to k_{obsd} given in eq 13. Fitting of the $k_{ob(1)}$ data to eq 13 leads to K_1 = 78.7 ± 6.2 M^{-1} and k_2 = 11.6 ± 0.4 s^{-1}, with $k_{ob(2)} = k_3$ = 0.96 ± 0.04 s^{-1}. In addition, fitting of the ΔA data of the initial fast change in absorbance to eq 5 results in K_1 = 97 ± 14 M^{-1}, which is in acceptable agreement with K_1 = 78.7 ± 6.2 M^{-1}, independently obtained from the dependence $k_{ob(1)} = f([H_2salen]_0)$.

The kinetic study of the substitution of the two bidentate ligands in complex II by H_2salen thus allows the observation and characterization of steps 1–3 (see eqs 9–11). Due to solubility problems, the kinetics of adduct formation according to step 1 could not be studied at a reduced temperature; the existence of equilibrium 9, as characterized by K_1, is a matter of fact however. It is worthwhile to point out that the rate of loss of the first bidentate ligand is higher than that of the second one ($k_2 \approx 12k_3$).

The kinetics of complex II reacting with H_2B = H_2[H_4]salen according to (2) are different in the sense that the conditions of case 4c are obviously fulfilled ($K_1[H_2B]_0 \gg 1$, k_2 and k_3 of comparable size). The greater nucleophilicity of H_2[H_4]salen compared to H_2salen shifts equilibrium 9 to completely form the adduct (step 1). As a consequence, the initial change in absorbance upon mixing, ΔA, is independent of $[H_2[H_4]salen]_0$ under the experimental conditions, and so are the two experimental rate constants, $k_{ob(1)}$ and $k_{ob(2)}$, of the biphasic substitution process according to steps 2 and 3 (see Figure 3). The evaluation of K_1 is thus impossible, and the assignment of $k_{ob(1)}$ = 0.015 ± 0.0003 s^{-1} and $k_{ob(2)}$ = 0.038 ± 0.001 s^{-1} to either k_2 or k_3 faces the slow–fast ambiguity.[22] The analysis of the experimentally obtained amplitudes a_1 and a_2 (see eq 7) allows however a clear assignment,[23,24] namely $k_{ob(1)} = k_2$ and $k_{ob(2)} = k_3$. In contrast to H_2salen, the hydrogenated ligand H_2[H_4]salen thus forms a much more stable adduct with complex II, the decay of which is by orders of magnitude slower. It is important to note that, under stoichiometric conditions ($[II]_0 = [H_2[H_4]salen]_0 = 2 \times 10^{-5}$ M) and at a slightly reduced temperature of 283 K, the second-order kinetics of adduct formation according to (9) are observable by stopped-flow spectrophotometry. Fitting of the A/t data to eq 8 leads to $k_1 = (5 \pm 0.1) \times 10^6$ M^{-1} s^{-1}.

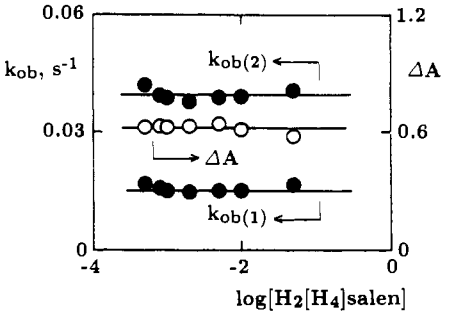

Figure 3. Plot of the initial fast change in absorbance, ΔA, and plot of the experimental rate constants, $k_{ob(1)}$ and $k_{ob(2)}$, vs the concentration of the entering ligand H_2[H_4]salen for complex II reacting according to eq 2 in acetone at 298 K ($[II]_0 = 4 \times 10^{-5}$ M).

The kinetics of the reaction of H_2BuMe[H_4]salen with complex II according to (2) seem to correspond to case 3, which means (i) fast and complete adduct formation according to step 1 with $\Delta A \neq f([ligand])$ and (ii) slow and ligand-independent product formation in one step with $k_{obsd} = k_2$ = 0.058 ± 0.002 s^{-1} at 298 K. There is no convincing explanation for step 3 not being observed.[25]

In conclusion, the reaction of complex II with H_2salen according to (2) follows case 4b and the parameters K_1, k_2, and k_3, characterizing steps 1–3 (eqs 9–11), are obtained (see Table II). The reaction of II with H_2[H_4]salen and H_2BuMe[H_4]salen is by several orders of magnitude slower. These ligands convert II to the corresponding adducts completely (step 1), and the rate of the subsequent steps 2 and 3 does not depend on the concentration of the incoming ligand.

Kinetic Results for Complex I Reacting with Ligands H_2B. The greater nucleophilicity of H_2[H_4]salen and H_2BuMe[H_4]salen compared to H_2salen led us to study the reaction of complex I according to (2) with both ligands at reduced and ambient temperature.

The solubility of I in acetone is sufficiently good to lower the temperature to 198 K. At this temperature the kinetics of adduct formation with H_2[H_4]salen according to step 1 (eq 9) can be studied under excess conditions ($[ligand]_0 \geq 10[I]_0$). As shown in Figure 4, the reaction is accompanied by a substantial blue shift from λ_{max} = 414 nm (I) to λ_{max} = 375 nm (adduct) and an increase in absorptivity, as observed for the formation of I·2py (Figure 1A) or I·Et$_2$en (Figure 1B) through spectrophotometric titration. The A_{375nm}/t data presented in Figure 4 can be well fitted with eq 6, which indicates pseudo-first-order kinetics. The

(21) The solubility of complex II is unfortunately very limited so that it was not possible to further lower the temperature.

(22) For an irreversible series of reactions A → B → C with a faster and a slower step, formal kinetics do not allow the discrimination between step A → B or step B → C being the faster or slower one. When spectrophotometric monitoring is used, this discrimination can be possible on the basis of the size of the absorptivity ϵ_B obtained for either assignment.[23]

(23) Alcock, N. W.; Benton, D. J.; Moore, P. *Trans. Faraday Soc.* **1970**, *66*, 2210.

(24) The slow–fast assignment results in a positive and sizewise meaningful value for the absorptivity of the postulated intermediate {Ni(Et-NO$_2$-sal)(H[H_4]salen)} ($\epsilon_{398} = (24 \pm 3) \times 10^3$ M^{-1} cm^{-1}), whereas the reverse assignment leads to a negative value ($\epsilon_{398} = -(4 \pm 0.6) \times 10^3$ M^{-1} cm^{-1}).

(25) The experiments were carried out under aerobic conditions so that the oxidative dehydrogenation of the product [Ni(BuMe[H_4]salen)][11] may have been unfavorably interfering.

Table II. Summary of Rate and Equilibrium Data for Reaction 2 Studied with Complexes I = $Ni(Et\text{-}sal)_2$ and II = $Ni(Et\text{-}NO_2sal)_2$ and Ligands H_2B in Acetone at 298 K

complex	H_2B	k_1, M^{-1} s^{-1}	K_1, M^{-1}	k_2, s^{-1}	k_3, s^{-1}	case
I	H_2salen		≤1[a]	86.1 ± 2.7[b]		1
I	$H_2[H_4]$salen	1160 ± 10[c]	897 ± 35[d] 637 ± 64[e]	0.12 ± 0.01	not obsd	2
I	H_2BuMe[H_4]salen	239.7 ± 1.5[c]	19.6 ± 0.8[d] 16.1 ± 1.5[e]	0.040 ± 0.001	not obsd	2
II	H_2salen		78.7 ± 6.2[d] 97 ± 14[e]	11.6 ± 0.4	0.96 ± 0.04	4b
II	$H_2[H_4]$salen	$5 \times 10^6 \pm 10^5$[f]	≥2×10^4[g]	0.015 ± 0.0003	0.038 ± 0.001	4c
II	H_2BuMe[H_4]salen		≥2×10^4[g]	0.058 ± 0.002	not obsd	3

[a] As estimated from $K_1[H_2B]_0 \leq 0.1$. [b] K_1k_2, M^{-1} s^{-1}, instead of k_2, as taken from ref 3. [c] At 198 K. [d] From the dependence $k_{obsd} = f([H_2B]_0)$ according to eq 13. [e] Calculated with eq 5 from the dependence of ΔA, the initial "jump" in absorbance, on $[H_2B]_0$. [f] Resulting from a stoichiometric kinetic run with $[II]_0 = [H_2[H_4]salen]_0 = 2 \times 10^{-5}$ M at 283 K. [g] As estimated from $K_1[H_2B]_0 \geq 10$.

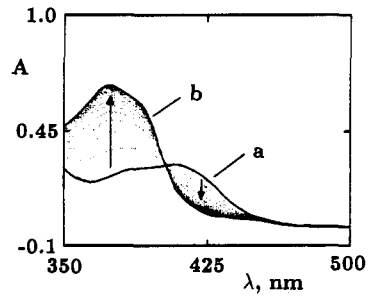

Figure 4. Spectral changes associated with the reaction of complex I (10^{-4} M) with $H_2[H_4]$salen (10^{-3} M) in acetone at 198 K: (a) $t = 0$; (b) $t = \infty$. The 15 spectra shown are part of 90 consecutive spectra in total, taken at time intervals Δt = 33 ms.

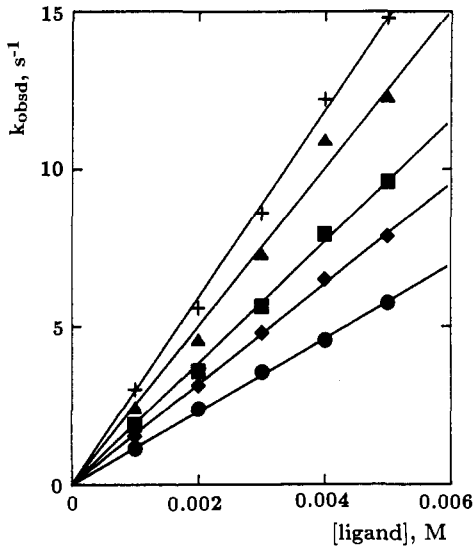

Figure 5. Plot of the experimental rate constant k_{obsd} for the reaction of complex I with the ligand $H_2[H_4]$salen in acetone at low temperature: 198 K, ●; 203 K, ◆; 208 K, ■; 213 K, ▲; 218 K, +.

study of this low-temperature adduct formation at variable ligand concentration and at different temperatures led to the data plotted in Figure 5. One recognizes that adduct formation in this system follows second-order kinetics with $d[adduct]/dt = k_1[I][H_2[H_4]$-salen] and k_1 = 1159 ± 10 M^{-1} s^{-1} at 198 K. The dependence $k_1 = f(T)$ yields the activation parameters $\Delta H^{\ddagger}$ = 15 ± 1.5 kJ mol^{-1} and $\Delta S^{\ddagger}$ = −106 ± 16 J mol^{-1} K^{-1} (see Table III). The negative entropy of activation is in line with the interpretation that the forward reaction of step 1 (eq 9) is a simple addition reaction.

Rate constant k_1 for adduct formation between I and $H_2[H_4]$-salen at room temperature is calculated to be 37.1×10^3 M^{-1} s^{-1}. This means that, under excess conditions ($[H_2salen]_0 = 50[I]_0 = 0.005$ M), the half-life for adduct formation at 298 K is about 4 ms. The kinetics of the addition reaction are therefore more or less lost within the mixing time of the stopped-flow apparatus and not reliably observable. The experimental result of fast adduct formation at room temperature is thus an initial "jump" in absorbance, ΔA, the size of which depends on the excess concentration $[H_2[H_4]salen]_0$. Fast adduct formation is followed by an exponential decay of the adduct spectrum to the product spectrum of [Ni([H_4]salen)] according to case 2. The dependence $k_{obsd} = f([H_2[H_4]salen]_0)$ is of the saturation type (see eq 13 and Figure 2B for $k_{ob(1)} = f([H_2salen]_0)$) and leads to k_2 = 0.12 ± 0.01 s^{-1} and K_1 = 897 ● 35 M^{-1}. Fitting of eq 5 to the $\Delta A/[H_2B]_0$ data results in K_1 = 637 ± 64 M^{-1}.

The reaction of complex I with the ligand H_2BuMe[H_4]salen resembles that with $H_2[H_4]$salen very much, which means (i) second-order adduct formation at low temperature (198 K), (ii) fast, nontraceable, and ligand-dependent adduct formation at ambient temperature according to equilibrium (9), as documented by a "jump" in absorbance, and (iii) monophasic product formation with $k_{obsd} = f([H_2BuMe[H_4]salen]_0)$ according to (13). So, this system is another example for the conditions of case 2 to be fulfilled. One learns from the comparison of the two ligands (see Table II) that the initially formed adduct with H_2BuMe[H_4]-salen (K_1 = 19.6 ± 0.8 and 16.1 ± 1.5 M^{-1}, respectively) is much less stable than that with $H_2[H_4]$salen and that its one-step decay to the product is slower (k_2 = 0.04 s^{-1}).

Temperature Dependence of Rate and Equilibrium Constants. Table III presents the activation parameters $\Delta H^{\ddagger}$ and $\Delta S^{\ddagger}$ for ligand substitution in complex I as well as the enthalpies ΔH° and entropies ΔS° for base addition.

The second-order reaction of I with $H_2[H_4]$salen to form the adduct (I·$H_2[H_4]$salen), as studied at low temperature, has a surprisingly low enthalpy of activation of only 15 kJmol^{-1}. As pointed out above, its strong negative entropy of activation is in line with a simple addition process. The decay of the adducts (I·$H_2[H_4]$salen) and (I·H_2BuMe[H_4]salen) with rate constant k_2, as studied at ambient temperature, is associated with a considerably higher enthalpy of activation (75 and 76 kJ mol^{-1}, respectively) and a small negative entropy of activation (−12 and −17 J mol^{-1} K^{-1}, respectively). The enthalpies of formation, ΔH°, of these two adducts (−70 and −63 kJ mol^{-1}, respectively), as obtained from the temperature dependence of the kinetically determined equilibrium constant K_1, are of approximately the same size as the enthalpies of activation. The corresponding entropies of formation, ΔS°, are strongly negative (−178 and −180 J mol^{-1} K^{-1}, respectively), which is to be expected for an addition reaction.

The data for ΔH° and ΔS° for base addition to complex I, as resulting from spectrophotometric titrations at variable temperature, are meaningful in comparison to the kinetically obtained ΔH° and ΔS° data for adduct formation. One recognizes that the coordination of two N atoms of the imine type (as is the case with 2 py, 2 PrBA, 1 bpy, or 1 PrPA) results in $\Delta H^{\circ} \approx -50 \pm 5$ kJ mol^{-1}, whereas the coordination of two secondary amine nitrogens (as in Et_2en) is associated with ΔH° = −69 ± 6.9 kJ mol^{-1}. Interestingly enough, the ΔH° data for the addition of $H_2[H_4]$salen and H_2BuMe[H_4]salen to complex I, as obtained kinetically, are clearly closer to −69 kJ mol^{-1} than to −50 kJ

Table III. Activation Parameters for Complex I = $Ni(Et\text{-}sal)_2$ Reacting with Ligands H_2B According to (2) and Thermodynamic Parameters for Base Addition to Complex I According to (4)

H_2B[a]	base[a] (denticity)	$\Delta H^{\ddagger}$, kJ mol^{-1}	$\Delta S^{\ddagger}$, J mol^{-1} K^{-1}	$\Delta H°$, kJ mol^{-1}	$\Delta S°$, J mol^{-1} K^{-1}
$H_2[H_4]$salen		15 ± 1.5[b]	−106 ± 16[b]		
$H_2[H_4]$salen		75 ± 7.5[c]	−12 ± 1.8[c]	−70 ± 7[d]	−178 ± 27[d]
H_2BuMe[H_4]salen		76 ± 7.6[c]	−17 ± 2.5[c]	−63 ± 6.3[d]	−180 ± 27[d]
	py (1)			−52 ± 5.2[e]	−146 ± 22[e]
	MeNBu (1)			−38 ± 3.8[f]	−118 ± 18[f]
	PrBA (1)			−19 ± 1.9[f]	−42 ± 6.3[f]
	PrBA (1)			−50 ± 5[e]	−130 ± 20[e]
	bpy (2)			−48 ± 4.8[f]	−108 ± 16[f]
	PrPA (2)			−52 ± 5.2[f]	−126 ± 19[f]
	Et_2en (2)			−69 ± 6.9[f]	−145 ± 22[f]

[a] For abbreviations, see footnote 5. [b] From the temperature dependence of k_1 at five temperatures in the range 198–218 K. [c] From the temperature dependence of k_2 at five temperatures in the range 293–313 K. [d] From the temperature dependence of K_1, obtained from $k_{obsd} = f([H_2B]_0)$ according to eq 13, at five temperatures in the range 293–313 K. [e] From the temperature dependence of β_2 (see Table I) at five temperatures in the range 293–313 K according to $\ln \beta = -\Delta H°/(RT) + \Delta S°/R$. [f] From the temperature dependence of K_1 (see Table I) as described in footnote *e*.

Table IV. Visible Absorption of the Adducts and/or Intermediates of Complexes I = $Ni(Et\text{-}sal)_2$ and II = $Ni(Et\text{-}NO_2sal)_2$ in Acetone at 298 K

species	λ_{max}, nm	ϵ_{max}, M^{-1} cm^{-1}
I	414	4 800
(I·MeNBu)[a]	378	8 000
(I·py)[a]	368	7 000
(I·2py)[a]	378	12 800
(I·PrPA)[a]	382	12 600
(I·bpy)[a]	386	12 600
(I·Et_2en)[a]	382	13 000
(I·$H_2[H_4]$salen)[b]	372[c]	12 900[c]
(I·$H_2[H_4]$salen)[b]	378[d]	12 660[d]
(I·H_2BuMe[H_4]salen)[b]	362	12 500
II	388	36 000
(II·py)[a]	390	44 700
(II·2py)[a]	392	47 700
(II·MeNBu)[a]	392	41 500
(II·2MeNBu)[a]	406	46 000
(II·Et_2en)[a]	406	45 500
(II·$H_2[H_4]$salen)[b]	403	47 000
(II·H_2BuMe[H_4]salen)[b]	392	45 000

[a] From spectrophotometric titration. [b] From kinetic studies. [c] At 198 K. [d] At 283 K.

mol^{-1}. This finding suggests that the addition of these tetrahydrosalen ligands occurs through the two N atoms.

Visible Absorption of the Adducts and/or Intermediates. To avoid confusion, a comment on the use of the terms "adduct" and "intermediate" is necessary. When reaction 2 is studied spectrophotometrically at ambient temperature and the A/t data obtained provide spectroscopic evidence ($\Delta A = f([H_2B]_0)$) and kinetic evidence ($k_{obsd} = f([H_2B]_0)$ according to eq 13) for the formation and involvement of a species ($Ni(R\text{-}sal)_2H_2B$), it is very adequate to call this species an "intermediate". It may be formed at low concentrations only, and it may be so labile that its isolation is impossible. The present study shows however that, at low temperatures, such an "intermediate" may become rather stable. The kinetics of its formation may be studied in detail and even its isolation may be possible, as in the case of $Ni(Et\text{-}sal)_2$(bpy).[20] This means that, depending on the experimental conditions, the "intermediate" ($Ni(R\text{-}sal)_2H_2B$), as formed to a minor extent by the addition of H_2B to $Ni(R\text{-}sal)_2$, may become a stable "adduct". In the mechanistic discussion of the present contribution, the term "adduct" will therefore be used for the species ($Ni(R\text{-}sal)_2H_2B$), to differentiate between an initially formed addition product and a possible intermediate such as (Ni(R-sal)HB), formed by elimination of the first bidentate ligand in the k_2 step (see eq 10).

Table IV summarizes the kinetically determined visible absorption characteristics of the various adducts ($I\cdot H_2B$) and ($II\cdot H_2B$) as well as those of the addition products obtained by titration with N-bases. The data provide information which is of value for the mechanistic discussion, namely (i) the addition of two monodentate N-donor ligands or of one bidentate N-donor ligand to I leads to a blue shift from 414 to about 380 nm and an absorptivity ϵ of about 12 800 M^{-1} cm^{-1}, (ii) the addition of a single monodentate N-donor ligand (such as py or MeNBu) also causes a similar blue shift, but the corresponding value for ϵ is much smaller, (iii) upon N-base addition to complex II, the analogous effects are observed, albeit less pronounced, and (iv) the absorption characteristics of the adducts ($I\cdot H_2B$) and ($II\cdot H_2B$), formed during the substitution process with $H_2B = H_2[H_4]$salen and $H_2B = H_2$BuMe[H_4]salen, are very close to those of the adducts (complex·2N-base) or (complex·N–N) (N–N = bidentate N-base).

The conclusion is therefore that the first step of ligand substitution according to (2) is the addition of the attacking ligands H_2B to the four-coordinate complexes I and II. The addition is such that the two N atoms in H_2B = HO–N–N–OH coordinate to form the six-coordinate, most probably octahedral species ($Ni(R\text{-}sal)_2$·HO–*N*–*N*–OH) (donating atoms italic). This result contrasts our earlier suggestion[3] that H_2B is coordinated in a monodentate fashion through formation of a single Ni–N bond, making the nickel center five-coordinate.

Mechanism of Ligand Substitution According to (2). The sum of kinetic, spectroscopic, and thermodynamic findings suggests a three-step mechanism for the substitution reaction (2), when studied under excess conditions ($[H_2B]_0 \gg [NiA_2]_0$). Depending on the nature of NiA_2 and H_2B, the kinetic investigation of the substitution process can reveal all three steps, (15)–(17), or just

$$Ni(O\text{–}N)_2 + HO\text{–}N\text{–}N\text{–}OH \underset{k_{-1}}{\overset{k_1}{\rightleftharpoons}} Ni(O\text{–}N)_2(HO\text{–}N\text{–}N\text{–}OH) \quad K_1 = k_1/k_{-1} \quad (15)$$

$$Ni(O\text{–}N)_2(HO\text{–}N\text{–}N\text{–}OH) \xrightarrow{k_2} Ni(O\text{–}N)(O\text{–}N\text{–}N\text{–}OH) + HA \quad (16)$$

$$Ni(O\text{–}N)(O\text{–}N\text{–}N\text{–}OH) \xrightarrow{k_3} Ni(O\text{–}N\text{–}N\text{–}O) + HA \quad (17)$$

part of them. For NiA_2 = II and $H_2B = H_2$salen, all three parameters are accessible, K_1, k_2, and k_3 (see Table II). For I reacting with $H_2[H_4]$salen and H_2BuMe[H_4]salen, respectively, the third step (eq 17) is obviously a fast consecutive reaction so that only K_1 and k_2 are obtained; in addition, however, rate constant k_1 for adduct formation is obtained. Complex II is such a strong Lewis acid that equilibrium 15 is completely shifted to the right for the two tetrahydrosalen ligands. As a consequence, only rate constants k_2 and k_3 or just rate constant k_2 is obtained. For complex I and the ligand H_2salen, finally, adduct formation is so weak that the kinetic study at ambient temperature yields just the composite parameter K_1k_2.

The spectroscopic and thermodynamic investigation of base addition to I and II provides conclusive information concerning

Scheme I. Possible Modes of Coordination in the Adducts Formed According to Equilibrium 15

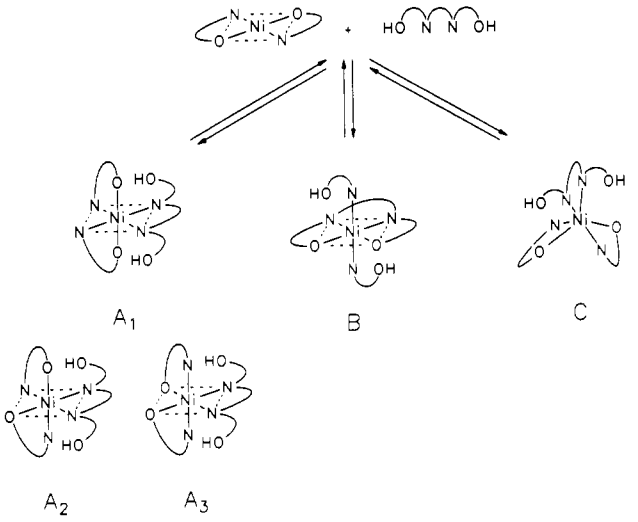

Scheme II. Mechanism Suggested for Ligand Displacement According to Steps 16 and 17

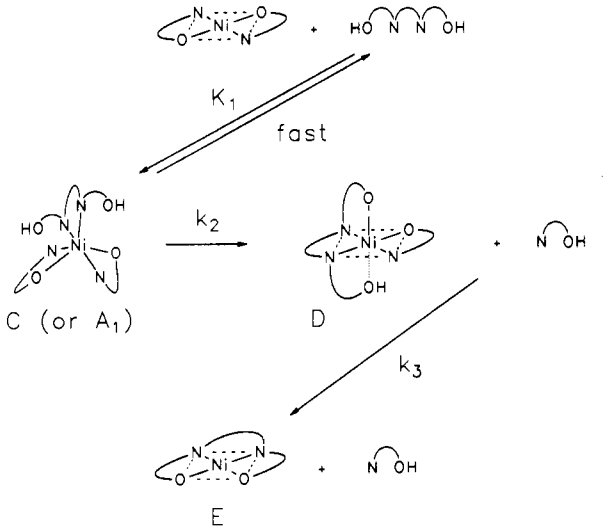

the state of coordination of the nickel in the adducts ($I \cdot H_2B$) and ($II \cdot H_2B$). The tetradentate tetrahydrosalen ligands HO–N–N–OH are doubly N-coordinated, thus making the nickel six-coordinate with an $(NO)_2N_2$ set of donor atoms. As shown in Scheme I, different modes of coordination are possible, A_1–A_3, B, and C. Taking into account the mode of coordination in the structurally characterized adduct Ni(E-sal)$_2$(bpy),[20] one has to favor structure A_1 with the four nitrogens forming a plane around the nickel and with the two oxygens of the salicylaldimine ligands being in axial positions. One has to admit however that a pseudooctahedral arrangement such as in C is a possible arrangement which cannot be excluded.

The establishment of equilibrium 15 is a fast process which is not rate-controlling at ambient temperature. The kinetic studies carried out at reduced temperatures confirm that the addition of H_2B to NiA_2 is a second-order reaction. Rate control at ambient temperature comes from reaction 16, in which the first bidentate ligand HO–N is eliminated from either C or A_1 after proton transfer from HO–N–N–OH to N–O$^-$. The state of coordination in the intermediate D thus formed (see Scheme II) is open to speculation. Unfortunately, the spectral changes associated with steps

$$C(\text{or } A_1) \xrightarrow{k_2} D \text{ and } D \xrightarrow{k_3} E$$

did not provide any conclusive information concerning possible changes in the state of coordination upon going from C (octahedral) to D and from D to E. The arrangement of donor atoms suggested in Scheme II for the intermediate D is a quasioctahedral one with the second phenolic OH group of the partially coordinated tetradentate ligand HO–N–N–O$^-$ being loosely attached.

Another open question is the relative size of first-order rate constants k_2 and k_3. For complex I, rate constant k_3 is not observed at all ($k_3 \gg k_2$). For complex II, both $k_2 > k_3$ (H_2B = H_2salen) and $k_2 < k_3$ (H_2B = H_2[H_4]salen) are found (see Table II). A convincing explanation for these findings is not at hand.

The results of the present study complement and extend the understanding of the mechanistic details of ligand substitution in planar four-coordinate nickel(II) complexes.[26] Pearson and Sweigart[27] investigated the kinetics of ligand substitution in bis(dithiolato)nickel(II) complexes by dithiolate nucleophiles[28] according to (18) in aqueous solution. In most cases, reaction

$$[Ni(S\text{–}S)_2]^{2-} + L\text{–}L^{2-} \rightleftharpoons [Ni(S\text{–}S)(L\text{–}L)]^{2-} + S\text{–}S^{2-} \quad (18)$$

18 followed second-order kinetics. For [Ni(*i*-mnt)(mnt)]$^{2-}$, however, and L–L = cpd^{2-}, saturation kinetics according to eq 13 were found for the formation of [Ni(mnt)(cpd)]$^{2-}$. The interpretation given by the authors corresponds to steps 15 and 16 of the present contribution, i.e., rapid (and spectrophotometrically detectable) formation of the adduct [Ni(*i*-mnt)(mnt)(cpd)]$^{4-}$ and subsequent decay to [Ni(mnt)(cpd)]$^{2-}$. The data led to the approximate values of K_1 = 270 and 170 M^{-1}, respectively. The authors postulate the adduct to be five-coordinate with the entering dithiolate ligand cpd^{2-} being bound in a monodentate fashion. This postulate is however not supported by a complete absorption spectrum of the adduct confirming five-coordination.

Conclusions

Planar four-coordinate complexes bis(*N*-alkylsalicylaldiminato)nickel(II) = Ni(R-sal)$_2$ = Ni(O–N)$_2$ are coordinatively unsaturated and add N-bases to become six-coordinate. The two bidentate ligands in Ni(O–N)$_2$ are readily displaced by tetradentate ligands HO–N–N–OH such as salen or tetrahydrosalen:

$$Ni(O\text{–}N)_2 + HO\text{–}N\text{–}N\text{–}OH \rightleftharpoons Ni(O\text{–}N\text{–}N\text{–}O) + 2\ HO\text{–}N$$

The mechanism of this substitution reaction is such that, first, HO–N–N–OH adds to Ni(O–N)$_2$ in a second-order reaction to form the six-coordinate octahedral adduct Ni(O–N)$_2$(HO–N–N–OH) with the tetradentate ligand being coordinated in bidentate fashion, surprisingly through the two N atoms of HO–N–N–OH. The size of the equilibrium constant for this adduct formation is governed by the Lewis acidity of the nickel center in Ni(O–N)$_2$ and by the basicity/nucleophilicity of HO–N–N–OH. Adduct formation is fast compared to the rate-controlling decay of the adduct, which is found to be monophasic (with loss of the first bidentate ligand being rate-controlling) or biphasic.

The system under study is one of the rare examples for associatively controlled substitution reactions in which the intermediate adduct can be thoroughly characterized by its absorption spectrum and by its thermodynamic and kinetic properties.

Acknowledgment. Sponsorship of this work by the Deutsche Forschungsgemeinschaft, Verband der Chemischen Industrie eV, and Otto-Röhm-Stiftung is gratefully acknowledged. Salicylaldehyde was kindly provided by Bayer AG.

(26) References 3 and 12 give a summary of references on the kinetics of ligand substitution in nickel(II) complexes.
(27) Pearson, R. G.; Sweigart, D. A. *Inorg. Chem.* **1970**, *9*, 1167.
(28) Abbreviations: mnt^{2-} = maleonitriledithiolate; *i*-mnt^{2-} = 1,1-dicyanoethylene-2,2-dithiolate; cpd^{2-} = 1-cyano-1-phenylethylene-2,2-dithiolate.